Available online at www.sciencedirect.com
SCIENCE DIRECT
International Journal of Pharmaceutics 315 (2006) 30–43
INTERNATIONAL JOURNAL OF PHARMACEUTICS
www.elsevier.com/locate/ijpharm

The protein-binding and drug release properties of macromolecular conjugates containing daptomycin and dextran

Walaisiri Muangsiri [1], Lee E. Kirsch *

Division of Pharmaceutics, College of Pharmacy, The University of Iowa, Iowa City, IA 52242, USA

Received 29 November 2005; received in revised form 8 February 2006; accepted 9 February 2006
Available online 20 March 2006

Abstract

Prototype daptomycin–dextran macromolecular conjugates were prepared in an attempt to modify the biodistribution and protein-binding properties of daptomycin. Synthesis of daptomycin macromolecular conjugates involved dextran activation, daptomycin–dextran coupling, and purification. The reaction mixtures were separated on a Sephadex G-100 column using 10% acetronitrile in water as a mobile phase. UV and fluorescence characteristics of high molecular weight fractions demonstrated imine product formation while the lower molecular weight fractions contained free daptomycin, imine, and anilide products. Daptomycin macromolecular conjugates were characterized by drug loading, drug release, and binding affinity for fibrinogen using HPLC analysis and surface plasmon resonance. Drug loading was calculated to be 160 mg of daptomycin per gram of macromolecule. Approximately 9% of the conjugated daptomycin was released from the macromolecular conjugates in aqueous media in the pH range of 1–7.4. The conjugates possessed higher affinity for fibrinogen than that of daptomycin.

Keywords: Aldehyde amine reaction; Surface plasmon resonance; Macromolecule; Drug loading; In vitro release; Peptide conjugation

1. Introduction

Bacterial endocarditis is a life-threatening disease. About 80% of endocardial infections are caused by Gram-positive organisms, primarily streptococci, enterococci, and staphylococci (Wilson et al., 1995). Successful antimicrobial treatment in endocarditis depends on drug penetration of the infection site (Bergeron, 1986). The emergence of vancomycin-resistant microorganisms has become a significant impediment to therapeutic success in treating this disease in the last 15 years (Murray, 2000).

Daptomycin is a lipopeptide antibiotic that has shown rapid in vitro bactericidal activity against glycopeptide-resistant pathogens and a unique mechanism of action compared with other classes of antibiotics. Initial daptomycin clinical trials for endocardial infections resulted in some treatment failures which may have been due to inadequate penetration of unbound drug into endocardial vegetations, rapid renal clearance, or extensive protein binding (Bergeron, 1986; Garrison et al., 1990; Lamp et al., 1992; Rybak et al., 1992; Lee et al., 1991). The use of dextran conjugates as macromolecular prodrugs for reducing toxicity, providing sustained drug release, or altering the biodistribution properties of various types of drug such as antibiotics and proteins has been reported (Battersby et al., 1996; Zhao et al., 1999; Kim et al., 2001; Yura et al., 1999). Recently a number of reports have shown that dextran derivatives have high affinity for fibrinogen which is the major component in cardiac vegetations (Retzinger et al., 1998; Retzinger and Deanglis, 1999; Sakamoto et al., 1999; Marchi et al., 2000). Dextrans (molecular weight >50 k) are retained in the blood circulation because of decreased glomerular filtration (Yura et al., 1999; Hemmelder et al., 1998). Thus, prototype macromolecular conjugates composed of daptomycin and dextran were evaluated in an effort to improve daptomycin efficacy in endocarditis by providing drug release rate and biodistribution.

Daptomycin, a potent lipopeptide antibiotic, is composed of 13 amino acid residues and a decanoyl side chain (Fig. 1; Debono et al., 1988). Daptomycin contains two primary amines

* Corresponding author. Tel.: +1 319 335 8824; fax: +1 319 335 9349.
E-mail addresses: walaisiri@yahoo.com (W. Muangsiri), lee-kirsch@uiowa.edu (L.E. Kirsch).
[1] Present address: Department of Pharmacy, Faculty of Pharmaceutical Sciences, Chulalongkorn University, Bangkok 10330, Thailand. Tel.: +66 2 218 8399; fax: +66 2 218 8401.

0378-5173/$ – see front matter © 2006 Elsevier B.V. All rights reserved.
doi:10.1016/j.ijpharm.2006.02.016

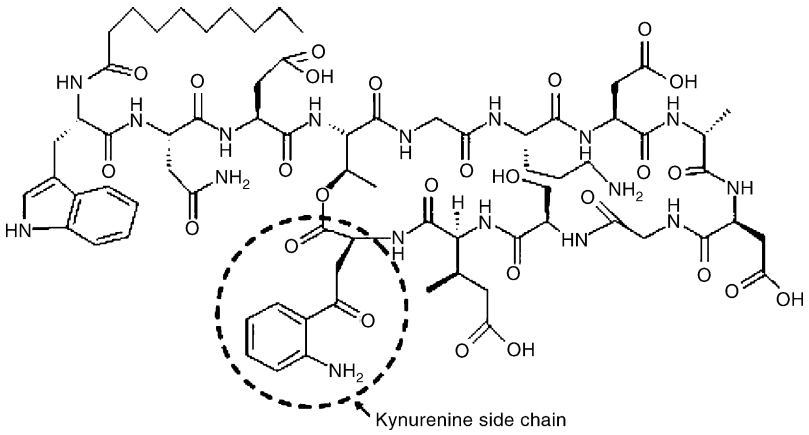

Fig. 1. Chemical structure of daptomycin.

(kynurenine and ornithine) and two fluorophores (tryptophan and kynurenine). Daptomycin is susceptible to hydrolytic degradation (Kirsch et al., 1989; Muangsiri and Kirsch, 2001). In a pH range of 0–14, daptomycin contains six ionizable groups including four carboxylic acid side chains (three aspartic acids and one methyl-glutamic acid) and two primary amines (kynurenine and ornithine). One of the carboxylic acid groups has a pK_a of 3.0 while the others have overlapping pK_a values at 5.3 (23 °C). pK_a values of the aromatic amine, kynurenine, is 0.8 whereas the aliphatic amine pK_a, ornithine, is 10. Daptomycin can spontaneously form reversible conjugates with reactive carbonyls such as reducing sugars (Inman and Kirsch, 1990). In the presence of glyceraldehyde, daptomycin forms Schiff's base and anilide products (Muangsiri et al., 2005). Thus, the formation of polysaccharide–drug conjugates utilizing carbonyl amine reaction was deemed probable.

As an antibiotic, daptomycin is bactericidal to most clinically significant Gram-positive microorganisms including vancomycin-resistant enterococci, methicillin-resistant staphylococci, and glycopeptide-intermediately susceptible *S. aureus*, coagulase-negative staphylococci and penicillin-resistant streptococci (Snydman et al., 2000; Rybak et al., 2000; Akins and Rybak, 2001). Its antibacterial effects are exerted on the bacterial cytoplasmic membrane. It disrupts membrane functions, including peptidoglycan synthesis, lipoteichoic acid synthesis, and the bacterial membrane potential. Its mechanism of action is distinct from that of other antibiotics, including β-lactams, aminoglycosides, glycopeptides, and macrolides (Boaretti et al., 1993; Alborn et al., 1991).

The bactericidal activity of daptomycin has been observed to be concentration dependent (Tally and DeBruin, 2000; Louie et al., 2001). Linear disposition and dose verus blood level area under the curve behavior has been reported (Woodworth et al., 1992). Glomerular filtration has been cited as the major route of daptomycin elimination (Rybak et al., 1992). Moreover, linear pharmacokinetic models have been used in the development of in vitro pharmacodynamic models (Bingen et al., 1991; Vance-Bryan et al., 1992) and animal infection models to describe daptomycin distribution and elimination kinetics (Michiels and Bergeron, 1996).

Initial clinical trials for the treatment of bacteraemia and soft tissue infections were successful, but treatment failures in bacterial endocarditis cases were observed (Garrison et al., 1990; Lamp et al., 1992; Lee et al., 1991). These failures were attributed to insufficient antibiotic concentrations at the infection site because of the insufficient antibiotic diffusion into the vegetations (Bergeron, 1986) and/or reduced free serum concentrations caused by extensive protein binding (Rybak et al., 1992; Lee et al., 1991). The increasing prevalence of serious infections caused by antibiotic-resistant Gram-positive bacteria has generated renewed interest in this agent's usefulness. In 1999 clinical trials were re-initiated to evaluate the intravenous administration of daptomycin for the treatment of serious Gram-positive infections and bacteraemia (Tally and DeBruin, 2000). Clearly, for the potential usefulness of daptomycin to be realized, drug delivery methodologies for generating high local concentrations of this potent antibiotic at the site of infection are needed.

The use of dextran conjugates as macromolecular prodrugs for reducing the toxicity, sustained release, or altering the biodistribution properties of various drugs has been reported. Recent studies have been conducted using ampicillin (Kim et al., 2001), the macrolide immunosuppresant: FK506 (Yura et al., 1999), 5-fluorouracil (Nichifor et al., 1995), epidermal growth factor (Zhao et al., 1999), recombinant human growth horman (Battersby et al., 1996), nystatin (Domb et al., 1996), and doxorubicin (Domb et al., 2000).

The prevalence of the use of dextran as a drug carrier is due, in part, to its worldwide use an effective and safe plasma volume expander in the intravenous treatment of shock caused by hemorrhage, burns or trauma (Mihara et al., 1994). Moreover, dextran is used to evaluate the molecular size-selective function of the glomerular filtration barrier. Typically, after intravenous administration, the distribution of poly disperse dextrans in plasma is compared to the size distribution of dextrans recovered in urine samples in order to determine the fractional renal clearance as a function of molecular size. Importantly, the fractional dextran clearance varies from about 0.8 for 20 kD dextran to $l < 0.01$ for 70 kD dextran which means that dextrans of sufficient molecular size are largely retained (Hemmelder et al., 1998). Thus, our proposal that the retention of macromolecular prodrugs based on

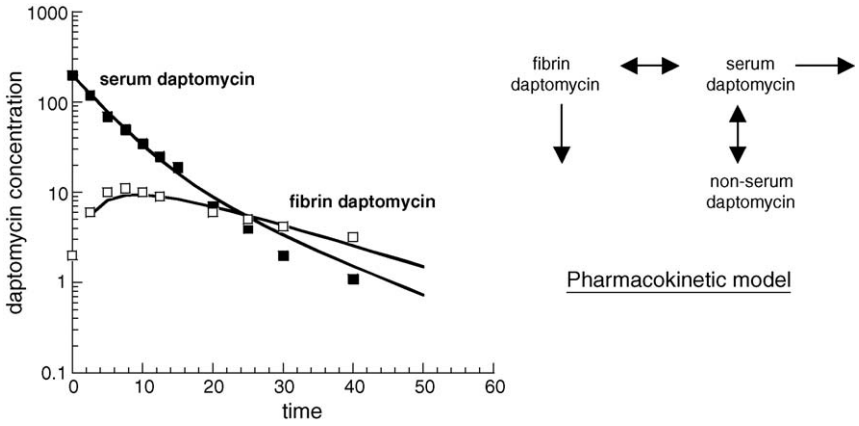

Fig. 2. Pharmacokinetic model for intravenous administration of daptomycin in a deep fibrin-embedded rabbit infection model. The open squares represent levels of daptomycin recovered from fibrin clots (mg/g) and the solid squares represent the corresponding serum daptomycin levels (mg/mL) after administration of 20 mg daptomycin/kg using a 30 min infusion (Michiels and Bergeron, 1996). Curves are pharmacokinetic model simulations.

size is a viable mechanism for decreasing their renal clearance (Dubrick and Wade, 1994).

Although dextran conjugates have not been described as a means of drug targeting (except for "passive targeting"; Harada et al., 2000), there have been a number of recent reports of high fibrin–dextran affinity, especially involving acidic dextrans such as dextran sulfate (Sakamoto et al., 1999) and carboxymethyl benzylamide sulfonate dextrans (Logeart-Avramoglou and Jozefonvicz, 1999). These reports tend to support our proposal that drug targeting to endocardial vegetation is feasible based on an enhanced affinity of daptomycin–dextran conjugates for fibrin.

The ultimate success of our approach depends on obtaining elevated levels of free daptomycin within fibrin vegetations. We have hypothesized that this objective can be accomplished using dextran–daptomycin macromolecular prodrugs by two mechanisms: decreasing the effective rate of drug elimination by retention of the macromolecular prodrug or drug targeting by increased prodrug–fibrinogen binding affinity. Pharmacokinetic simulations were used to test whether our hypotheses were reasonable.

A pharmacokinetic model for the time course of daptomycin in serum and fibrin clots was developed using published data on the disposition of intravenously administered daptomycin in a deep fibrin-embedded rabbit infection model (Michiels and Bergeron, 1996). The model accounted for biexponential disposition of serum daptomycin and the appearance and loss of drug in fibrin clots. As can be observed in Fig. 2, the agreements between the reported drug levels and the curves representing pharmacokinetic model simulations were very good thus indicating that the model adequately describes the time course of daptomycin in both tissues after intravenous administration of drug. Based on literature reports, the use of a linear pharmacokinetic model is appropriate for daptomycin (Rybak et al., 1992; Woodworth et al., 1992).

This model was expanded to describe free daptomycin fibrin levels obtained from the intravenous administration of macromolecular prodrug delivery systems by assuming that the rate constants for prodrug reversal to free daptomycin in serum and the fibrin clot were the same, that the total amount of drug was equivalent to that used in the published rabbit model data, and that the apparent serum volume of the prodrug and drug were equal. The key distributional processes (e.g. prodrug reversal, fibrin affinity, and renal clearance) are explicitly depicted in Fig. 3 where the kinetics of prodrug drug reversal, drug and prodrug fibrin affinity, and drug and prodrug elimination are represented by PR, FA, and RE, respectively.

The effects of varying each key biodistributional process were studied by simulating a reasonable range of kinetic parameters associated with each key process and comparing the resulting free fibrin daptomycin concentration time profiles (labeled *fibrin daptomycin* in Fig. 3) to the reported drug levels in fibrin following intravenous administration of drug.

As shown in Fig. 4 by comparing curve a to the solid circles, rapid prodrug reversal ($t_{1/2} = 1$ h) results in fibrin drug levels equivalent to intravenous daptomycin administration. Increasing the prodrug reversal half-life from 10 to 40 h (curves b–d in Fig. 4) resulted in reduced fibrin drug levels. Thus our analysis is in agreement with previous reports (Bergeron, 1986) that sustained drug delivery alone will not provide the elevated fibrin

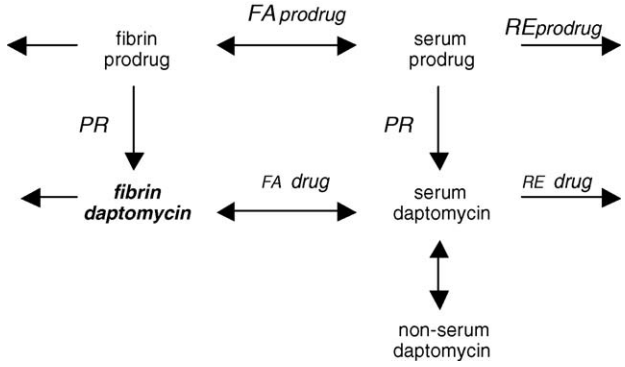

Fig. 3. Extended pharmacokinetic model for predicting fibrin daptomycin levels after the intravenous administration of macromolecular prodrugs. The rate of daptomycin appearance from the prodrug is described by the processes labeled PR, whereas prodrug/daptomycin fibrin affinity process is labeled FA and renal elimination process is labeled RE.

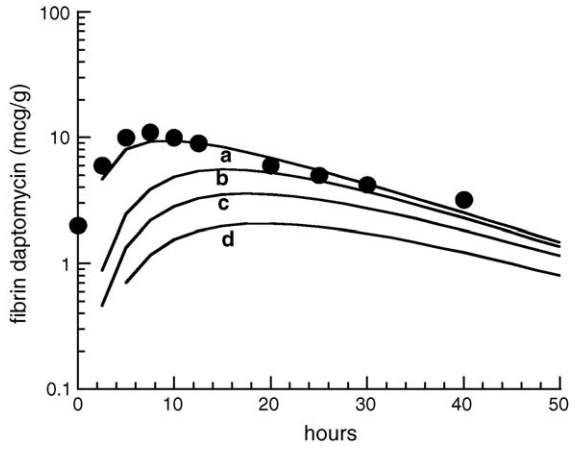

Fig. 4. The effect of prodrug reversal rates on the free fibrin daptomycin concentration time profiles simulated using a pharmacokinetic model developed from a deep fibrin-embedded rabbit infection model (Michiels and Bergeron, 1996). The solid circles represent data obtained from administration of 20 mg daptomycin/kg using a 30 min infusion (Inman and Kirsch, 1990). Curves are simulations using the prodrug pharmacokinetic model (Fig. 2) in which the prodrug reversal half-life was 1 h (curve a), 10 h (curve b), 20 h (curve c) or 40 h (curve d).

drug levels needed for effective antibiotic therapy of deep tissue infections.

Contrariwise, decreasing the kinetics of prodrug elimination or increasing prodrug affinity for fibrin beyond that associated with the parent drug resulted in increased free drug levels within fibrin clots. For example as illustrated by the hatched and solid gray bars in Fig. 5B, the drug fibrin levels predicted by the administration of macromolecular prodrugs with elimination half-lives two- to four-fold greater that the parent drug were 150–200% of the drug fibrin levels obtained from intravenous administration of the parent drug. The magnitudes of the renal disposition changes simulated herein are consistent with the reported changes for macromolecular conjugates (Dubrick and Wade, 1994).

The predicted effects of increased prodrug fibrin affinity on free daptomycin levels in fibrin clots were also profound. For example the solid bars in Fig. 5A illustrate the effects of an eight-fold increase on prodrug fibrin affinity wherein the free daptomycin fibrin levels at five hours are 150% and continue to increase to over 300% of those obtained by intravenous administration of the parent drug. Taken together, our simulations illustrate that variations in the distributional properties of the proposed macromolecular prodrug delivery system may result in significant improvements in daptomycin penetration into fibrinous endocardial vegetations.

Macromolecular conjugates of daptomycin and dextran in the treatment of bacterial endocarditis may overcome the poor penetration of the parent drug into infected tissues and its rapid renal clearance. The key factors are three-fold. Firstly, the spontaneous and reversible reactions between the primary amine of daptomycin and carbonyls of modified dextran are chemically feasible. Secondly, renal clearance of the macromolecular conjugates can be manipulated by choosing the proper molecular weight of dextran. Finally, drug targeting may result from a high affinity for fibrinogen of dextran-based macromolecular conjugates.

The main objectives of this work were to synthesis daptomycin–dextran macromolecular conjugates and characterize the conjugates including the measurement of the in vitro drug release and fibrin-binding properties using surface plasmon resonance (SPR).

2. Experimental

2.1. Daptomycin HPLC analysis

The HPLC system consisted of a pump (Shimadzu LC-6A), an integrator (HP 3395), an UV detector (Shimadzu SPD-6AV), an autoinjector (Water 712 WISP). The HPLC method was adapted from a previously reported method (Kirsch et al.,

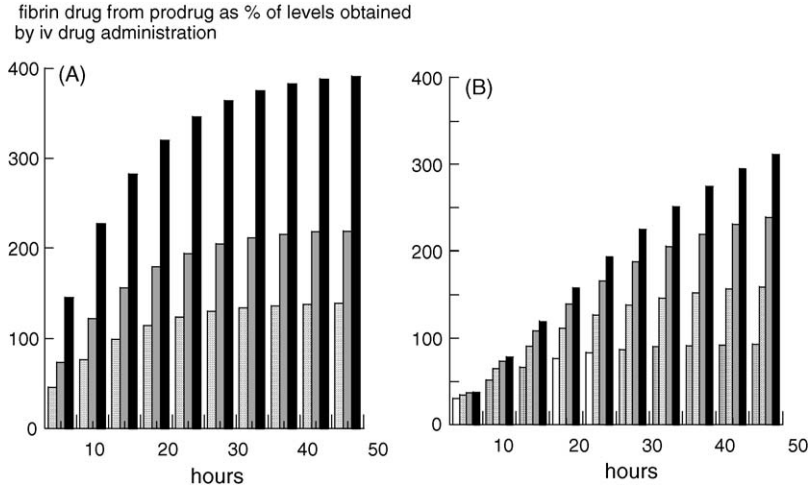

Fig. 5. The effects of prodrug fibrin affinity (A) and elimination (B) on the relative free daptomycin levels in fibrin clots. In each figure the effects of variations in the prodrug dispositional properties were depicted by comparison to the daptomycin fibrin levels described by the model depicting intravenous administration of daptomycin. (A) The prodrug affinity was increased over that of daptomycin by a factor of two (hatched bars), four (solid gray bars) and eight (solid black bars). (B) The prodrug elimination was equal to daptomycin (open bars) or decreased by a factor of two (hatched bars), four (solid gray bars) or eight (solid black bars). In all prodrug model simulations the reversal half-life was 10 h.

1989) and employed a 250 mm × 4.6 mm i.d., 5 μm particle size, C-8 column (Zorbax 300SB-C8, Hewlett Packard®, Serial# HD2411). The column was operated at room temperature using a solvent flow rate of 1 mL/min. The mobile phase was acetonitrile:0.05 M phosphate buffer, pH 5 (29:71). The sample injection volume was 10 μL, and the runtime was 30 min. Daptomycin and related substances were detected at a wavelength of 214 nm, 0.64 AUFS. The column was stabilized at least 3 h prior to use. A typical chromatogram revealed peaks at retention times of 17, 16, and 24 min corresponding to daptomycin, β-asp daptomycin, and anhydrodaptomycin, respectively. Typical four point calibration curves, peak areas versus concentration, were linear ($R^2 > 0.99$) in the concentration range of 0.02–0.3 mM. The samples were diluted with double distilled water if necessary.

2.2. Dextran activation

The periodate method was employed to oxidize dextran of various average molecular weights, (6000, 40,000, and 110,000). The reaction scheme for dextran activation is depicted in Fig. 6A. A 50 mg/mL dextran solution in distilled water was oxidized by addition of solid sodium metaperiodate. The reaction was allowed to proceed at room temperature in the dark. The reaction was quenched by an addition of excess ethylene glycol. The solution was dialyzed against distilled water using dialysis membrane with molecular weight cut off 100 and lyophilized using a shelf freeze dryer (Virtis AdVantage) prior to further studies. The presence of aldehyde groups in activated dextran was determined using a modified hydroxylamine hydrochloride method (Zhao, 1991). Unreacted dextran samples were used as controls.

A series of experiments was conducted to evaluate the effects of reaction duration, periodate concentration, and dextran molecular weight on number of aldehyde substitutions (Table 1).

2.3. Determination of activated functional groups on dextran

Approximately 100 mg of lyophilized activated dextran was weighed and dissolved in 25 mL of 0.25N hydroxylamine hydrochloride solution (pH 4.0). The solution was placed on the bench top at room temperature for at least 2 h to allow the reaction to be completed. The solution was potentiometrically titrated with standardized 0.1N sodium hydroxide solution to pH 4.0. A magnetic stirrer was employed to obtain a uniform solution during the titration. The number of aldehyde substitutions per 100 glucose subunits was estimated from the amount of standardized 0.1N sodium hydroxide used in the titration using the following equation:

$$\text{aldehyde per 100 glucose subunits} = N \times V \times \frac{\text{MW}}{\text{wt}} \times \frac{100}{S} \quad (1)$$

where N is the concentration of standardized sodium hydroxide, V volume in milliliters used in the titration, MW the molecular weight of dextran, wt weight in grams of dextran, and S is the number of subunits in activated dextran.

2.4. Daptomycin-activated dextran 40 coupling

A coupling reaction between 0.015 M daptomycin and activated dextran containing 0.16 M aldehyde groups was performed in a pH range of 2–5. A scheme for the coupling of activated dextran and daptomycin based on the known reaction between daptomycin and glyceraldehyde (Muangsiri et al., 2005) is depicted in Fig. 6B. The activated dextran was determined to have approximately 27 aldehyde groups per 100 glucose subunits. The lyophilized activated dextran was dissolved in distilled water at a pre-equilibrated temperature of 25 °C. Daptomycin was added to initiate the coupling reaction. The reaction solution was adjusted

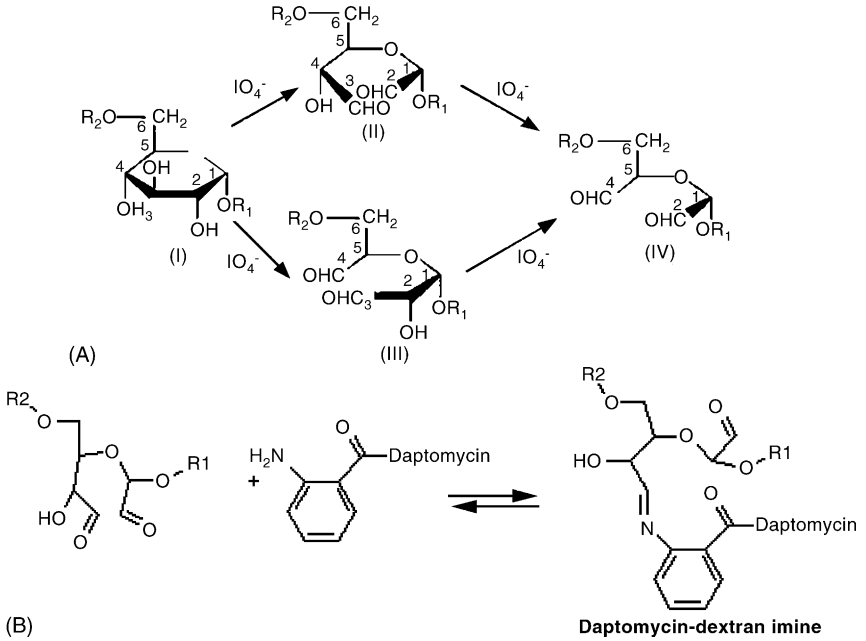

Fig. 6. Reaction schemes. (A) Formation of activated dextran using the periodate method. (B) Formation of daptomycin–dextran conjugates by the reaction of aldehydic dextran residues and the aromatic side chain of kynurenine residue in daptomycin to give rise to an imine.

Table 1
Experimental conditions used to evaluate parameters effecting number of aldehyde substitutions in activated dextran

Reaction number	MW of dextran	Periodate:glucose subunit (molar ratio)	Reaction time (h)	Number of aldehyde substitution/100 glucose subunit* average + S.D. ($n = 3$)
1	Dextran 6000	0.15	1–24	18.9 ± 0.2
2	Dextran 6000	0.29	1	37.7 ± 0.7
3	Dextran 6000	0.59	1	85.7 ± 0.5
4	Dextran 6000	1.2	1	186 ± 1
5	Dextran 6000	1.5	1	254 ± 0
6	Dextran 6000	1.7	1	265 ± 2
7	Dextran 6000	2.0	1	295 ± 8
8	Dextran 6000	2.5	1	295 ± 4
9	Dextran 40,000	0.022	1–24	3.60 ± 0.01
10	Dextran 40,000	0.044	1	6.65 ± 0.02
11	Dextran 40,000	0.089	1	13.5 ± 0.1
12	Dextran 40,000	0.18	1	27.1 ± 0.0
13	Dextran 110,000	0.0090	1–24	1.63 ± 0.03
14	Dextran 110,000	0.018	1	2.95 ± 0.02
15	Dextran 110,000	0.035	1	5.78 ± 0.06
16	Dextran 110,000	0.071	1	11.2 ± 0.1

to the desired pH by addition of standardized hydrochloric acid or sodium hydroxide. The reaction temperature was controlled using a water bath. Aliquots were withdrawn at appropriate time intervals and immediately analyzed for depletion of unconjugated daptomycin in the reaction mixture using HPLC analysis. Loss of daptomycin in distilled water at 25 °C was monitored as a control study. For each reaction solution, pH values at the initial and final time point were insignificantly changed.

Separation of daptomycin-activated dextran conjugates was achieved by gravitational gel filtration chromatography using Sephadex G-100 as a stationary phase and 10% acetonitrile in water as a mobile phase. Fractions were collected using an Eldex fraction collector. The presence and spectral characteristics of daptomycin and daptomycin-activated dextran macromolecular conjugates were determined by a HP 8453A UV spectrophotometer (using an analytical wavelength of 365 and 377 nm, respectively) and fluorescence spectroscopy using excitation and emission wavelengths of 364 and 465 nm, respectively. Free daptomycin and activated dextran were used as reference standards of known molecular weights. Upon completion of the separation, appropriate fractions containing high molecular weight conjugates were lyophilized for further evaluations.

2.5. Determination of drug loading

The amount of conjugated daptomycin was determined by dissolving a known amount of conjugates in aqueous media. Total daptomycin and free daptomycin concentrations in the macromolecular aliquots were determined by UV absorbance at 282 nm and HPLC at the analytical wavelength of 214 nm, respectively. The difference between the total and unconjugated daptomycin concentrations in the sample equaled the concentration of conjugated daptomycin. Drug loading was expressed as the mass of conjugated daptomycin per gram of macromolecular conjugate. The conjugation efficiency was determined as the number of moles of aldehyde groups occupied by one molecule of daptomycin.

2.6. In vitro drug release

The release rate of daptomycin from the macromolecular conjugates prepared at pH 2 was determined in aqueous media in the pH range of 1–7.4 at 60 °C by HPLC analysis. A known amount of the conjugate was dissolved in buffered media (Table 2). The pH of the release medium was determined at the beginning and at the end of the studies. Degradation of free daptomycin and activated dextran alone under the same experimental conditions was determined and used as control studies. Solution aliquots were removed periodically and the free daptomycin concentration was determined.

2.7. Fibrinogen binding studies

SPR experiments were performed to determine the affinity of daptomycin or daptomycin conjugates for fibrinogen. The experimental procedures included immobilization of fibrinogen, evaluation of mass transfer effects and determination of interaction between daptomycin or daptomycin conjugates and human fibrinogen.

2.8. Immobilization of fibrinogen

Human fibrinogen was immobilized over the activated surface of the CM5 Sensor Chip using a method developed by Sakamoto et al. (1999). Sorensen's buffer (PBS) pH 7.4 was used as a running buffer. A 70 μL volume of an equimolar mixture of *N*-ethyl-*N*′-(dimethylaminopropyl) carbodiimide HCl (EDC) and *N*-hydroxysuccinimide (NHS) was passed over the

Table 2
Experimental conditions for release studies of macromolecular conjugates using HPLC analysis at 60 °C (μ = 0.154 M)

Reaction number	Material	Release medium	Daptomycin initial concentration (mM)	Initial PH
1	Conjugates pH 2	0.100 M hydrochloric acid, pH 1.0	0.521	1.16
2		0.200 M acetate buffer, pH 4	0.492	1.20
3		0.0550 M phosphate, buffer, pH 7.4	0.462	1.20
4	Daptomycin	0.100 M hydrochloric acid, pH 1.0	0.538	4.07
5		0.200 M acetate buffer, pH 4.0	0.437	4.08
6		0.0550 M phosphate, buffer pH 7.4	0.610	4.13
7	Activated dextran	0.100 M hydrochloric acid, pH 1.0	0.563	7.42
8		0.200 M acetate buffer, pH 4.0	0.517	7.42
9		0.0550 M phosphate buffer, pH 7.4	0.499	7.51

carboxymethyldextran sensor chip surface to modify carboxy groups of the matrix to *N*-hydroxysuccinimide esters. A 5 μL volume of human fibrinogen (400 μg/mL) in 10 mM acetate buffer, pH 5.0, was passed over the CM5 sensor chip. The *N*-hydroxysuccinimide ester was replaced and formed amide bonds with unprotonated amine groups of the ligand. The remaining activated surface was then blocked by a 7 min flow of ethanolamine at a flow rate of 10 μL/min. A continuous flow of PBS buffer (pH 7.4) was passed over the sensor chip prior to conduct further experiments. Approximately 2400 resonance units (RU) of fibrinogen were immobilized on the sample flow cell of sensor chip at the end of the immobilization process. The surface of the reference flow cell was treated as mentioned above without exposure to human fibrinogen. Phosphate buffer (0.064 M, pH 7.4, $\mu = 3$ M) was used as a regeneration solution.

2.9. Evaluation of mass transfer effects

The reference and sample flow cells were exposed to 20 μL of 20 μM daptomycin using various flow rates ranging from 5 to 50 μL/min to evaluate the presence of mass transfer effects. Response from the active flow cell was subtracted from that of the reference flow cell to eliminate non-specific binding between analyte and the sensor chip surface. The elapsed time between signals obtained from both flow cells was adjusted. The difference in response units was plotted to depict the mass transfer effect. The association phases of the sensorgrams at various flow rates were superimposable. Thus, the mass transfer effect was insignificant at a flow rate faster than 5 μL/min.

2.10. Interaction of daptomycin or conjugates with human fibrinogen

A 20 μL volume of 200 nM of either daptomycin or daptomycin macromolecular conjugates in PBS buffer was brought into contact with the sensor chip (CM5). The flow rate was kept at 10 μL/min. At the end of the sample exposure, PBS buffer was passed over the sensor surface to allow dissociation. After a suitable dissociation, the sensor surface was regenerated for the next sample using 10 μL of regenerating buffer. After background subtraction, the kinetic models were fitted to sensorgrams using BIAevaluation 3.1 by BIACore International AB (Neuchâtel, Switzerland) to determine dissociation and association rate constants and the dissociation constant (K_d).

3. Results and discussion

Daptomycin has been shown to react with aldehyde containing compounds such as D-glucose and glyceraldehyde (Inman and Kirsch, 1990; Muangsiri et al., 2005). In this study, the reaction between unprotonated primary amine of daptomycin and aldehyde of activated dextran was utilized to synthesize daptomycin activated dextran macromolecular conjugates at the coupling pH values of 2–5. The conjugates were purified and characterized by fibrinogen binding and drug release properties.

3.1. Dextran activation

A series of experiments were conducted to evaluate the effects of reaction duration, periodate concentration, and dextran molecular weight on the number of aldehyde substitutions.

The effect of reaction duration on the number of aldehyde substitutions was determined by monitoring the number of aldehyde substitutions as a function of time for 24 h (reactions 1, 9, and 13 in Table 1). Moles of aldehyde substitutions per 100 glucose subunits were increased from 2.60, 0.33, and 0.35 to 145.66, 23.82, and 10.93 for dextran 6000, 40,000, and 110,000, respectively, within 1 h after the reaction was initiated. Since there was no significant increase or decrease in the number of aldehyde substitutions after 1 h upto 24 h of reaction duration, the number of aldehyde substitutions did not depend on reaction duration (>1 h).

The effect of periodate concentration on the number of aldehyde substitutions was studied in a concentration range of 0.15:1 to 2.5:1 molar ratio of periodate : glucose subunit (reaction # 1–8, Table 1). The number of aldehyde substitutions per 100 glucose subunits linearly increased from 4.97 to 254.42 moles as the periodate concentration increased from 0:1 to 1.5:1 molar ratio of periodate: glucose subunits with a slope of 172 (Fig. 7, inset). In other words, every molecule of periodate, on average, created 1.7 aldehyde groups per glucose subunit. The number of aldehyde substitutions slowly increased and leveled off at 295 moles of aldehyde per 100 glucose subunits when the periodate concentration was higher than 1.5 molar ratio of periodate : glucose subunits.

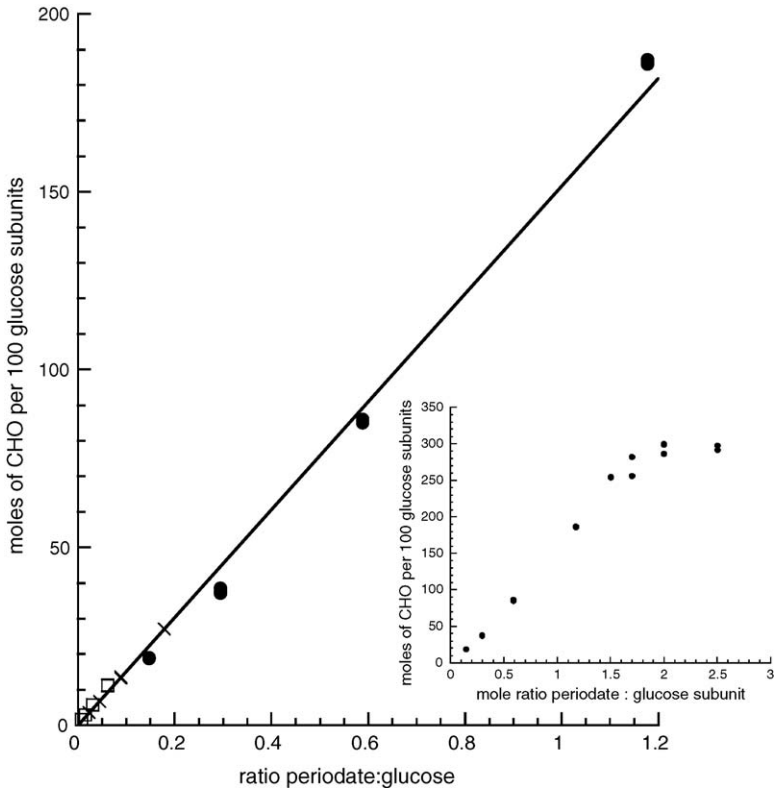

Fig. 7. Effect of dextran molecular weight on periodate oxidation. Dextran 6000 (●), 40,000 (×), and 110,000 (□) were oxidized at room temperature in the dark for 1 h and number of aldehyde substitutions was determined using the hydroxylamine HCl method. Insert shows effect of periodate concentration on number of aldehyde substitutions on lyophilized-activated dextran 6000 after the reaction was conducted at room temperature in the dark for 1 h.

The effect of dextran molecular weight was studied by oxidation of dextran 6000, 40,000, and 110,000 with 0.009:1 to 1.176:1 moles of periodate : moles of glucose subunits (reaction# 1–4 and 9–16, Table 1). The number of aldehyde substitutions linearly increased as the concentration of periodate per glucose subunit of dextran increased with slopes of 164.7, 151.6, and 179.2 for dextran 6,000, 40,000, and 110,000, respectively (Fig. 2). Thus, the number of aldehyde substitutions in activated dextran was independent of the nominal size of the dextran substrate and was constant at approximately 165 aldehyde groups per 100 glucose subunits consistent with the previous result (one molecule of periodate created 1.7 aldehyde groups on one glucose subunit).

3.2. Daptomycin-activated dextran coupling reactions

The initial loss of daptomycin concentration in the presence of activated dextran was 50-fold faster than loss rate of daptomycin in absence of activated dextran at 25 °C (Fig. 8). Up to 90% of free daptomycin was lost within 120 h due to conjugate formation. First-order plots showed biphasic characteristics perhaps due to complex reversible reactions. The apparent rate of daptomycin loss due to conjugation was pH independent. In the absence of activated dextran, daptomycin (pH 4) slowly degraded and formed anhydrodaptomycin and β-asp daptomycin which was consistent with previously reported data (Kirsch et al., 1989).

3.3. Separation of macromolecular conjugates on sephadex G-100 using an aqueous mobile phase and average molecular size determination

The use of 0.10 M phosphate buffer, pH 7.2, as an aqueous mobile phase was initially investigated with 0.5 mL aliquots

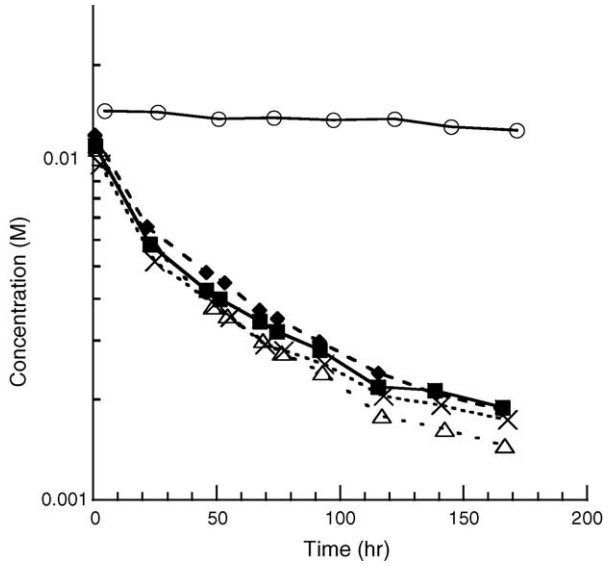

Fig. 8. First-order plots of unconjugated daptomycin in the absence of activated dextran pH 4 (◯), and unconjugated daptomycin in the presence of activated dextran at 25 °C pH 1.97 (■), 2.84 (♦), 4.12 (×), and 5.24 (△).

of 1.2 mM daptomycin, or 1.33 mM daptomycin-activated dextran conjugates. The Sephadex G-100 column was calibrated using five known protein markers at an analytical wavelength of 282 nm. The presence of daptomycin and daptomycin-activated dextran conjugates in each fraction were determined based on UV absorbance at 365 and 377 nm, respectively. The percent recovery was also determined.

Free daptomycin has UV absorption maxima at 282 or 365 nm corresponding to the UV maxima of tryptophan and kynurenine residues, respectively. Upon conjugation of daptomycin to activated dextran, the 365 nm maximum shifted to 377 nm while the 282 nm peak remained unchanged. Thus, the concentration of daptomycin present as conjugate was estimated using the tryptophan UV absorbance at 282 nm.

The elution profile of a mixture of five marker proteins showed five well separated peaks with elution volumes of 29, 34, 48, 60, and 79 mL corresponding to thyroglobulin (MW 670,000), bovine gamma globulin (MW 158,000), chicken ovalbumin (MW 44,000), equine myoglobin (MW 17,000), and vitamin B12 (MW 1350), respectively.

The elution profile of a 0.5 mL aliquot of 1.2 mM daptomycin showed a single peak with an elution volume of 80 mL which was approximately equivalent to that of Vitamin B12 (MW 1350). This result was consistent with the fact that the molecular weight of daptomycin is 1620. The total amount of daptomycin present in this fraction was determined by measurement at the tryptophan UV absorbance maximum to be 0.842 mg which was 86.4% recovery of the total daptomycin contained in the 0.5 mL aliquot.

The elution profile of 0.5 mL aliquot of 1.33 mM daptomycin–dextran conjugate showed three major broad peaks corresponding to elution volumes of 28, 40, and 83 mL. The peaks at elution volumes 28 and 40 mL indicated the presence of high molecular weight compounds corresponding to molecular weight of >100 and 93 k, respectively. Total amount of daptomycin present in the fractions was 0.97 mg or 84% recovery of the total daptomycin contained in the 0.5 mL aliquot. Furthermore, the percent unconjugated daptomycin (determined from the peak at elution volume 80 mL) was 27.0% which was in general agreement with the percent recovered using HPLC analysis (23%).

3.4. Separation of macromolecular conjugates on sephadex G-100 using 10% acetonitrile in water as a mobile phase and average molecular size determination

Typically, aqueous salt solutions are used as mobile phases in gel filtration chromatography. Ionic strength is adjusted to minimize adsorption and interactions between the eluent and the stationary phase. However, co-solvents can be used as a mobile phase to optimize the separation or to overcome problems due to solubility or adsorption of the eluent. In this study, separation of macromolecular conjugates on a Sephadex G-100 gel filtration chromatography column with a 80 mL bed volume at room temperature using 10% acetonitrile in water as a mobile phase was investigated in order to minimize adsorption of daptomycin or daptomycin-activated dextran conjugates.

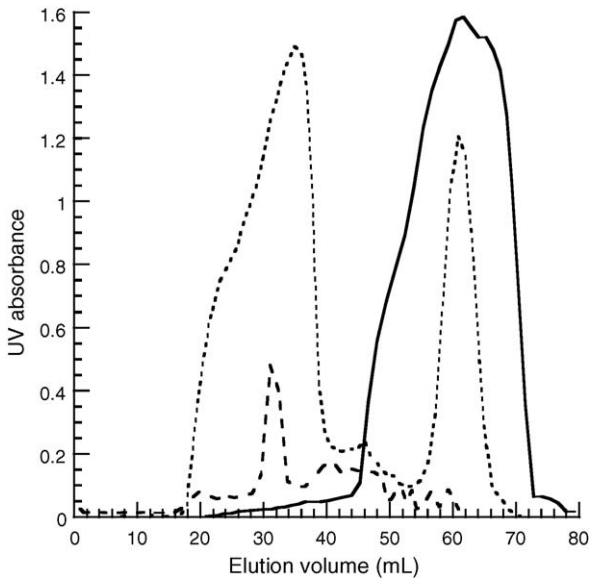

Fig. 9. Elution profile of 0.5 mL 0.015 mM daptomycin (—), 0.5 mL activated dextran containing 0.158 M aldehyde groups (- - -), and 0.5 mL of 1 mM daptomycin and 2.5 mM activated dextran mixture coupled at pH 2 (· · ·) on Sephadex G-100 using 10% acetonitrile as a mobile phase. The presence of daptomycin, activated dextran, and daptomycin conjugates in each fraction was determined by UV absorbance at 365, 220, and 377 nm, respectively.

The Sephadex G-100 column using 10% acetonitrile in water as a mobile phase was calibrated using 5 marker proteins. The elution profile of the marker proteins showed three distinct peaks with elution volumes of 33, 60, and 70 mL. A shoulder was observed for the peak at the elution volume of 60 mL indicating of co-elution of some marker proteins. This likely occurred because of protein denaturation in the presence of the non-aqueous solvent. Thus, the Sephadex G-100 column could not be calibrated using the five marker proteins.

Compounds of known molecular weight, i.e. 0.015 M free daptomycin and activated dextran containing 0.158 M aldehyde groups, were used as molecular weight standards (Fig. 9). The elution profile of daptomycin showed one broad peak with an elution volume of about 60 mL while the elution profile of activated dextran showed one major peak with an elution volume of 31 mL. Therefore, fractions with elution volume equal to or less than 30 mL were estimated to have molecular sizes $\geq$40,000. Fractions with elution volume equal to 60 mL were estimated to have molecular size $\approx$ 1600. The percent recovery was determined to be 90.1% from the total amount of daptomycin recovered from (11.57 mg) and the theoretical amount of daptomycin (12.84 mg) applied on the gel column using co-solvent mobile phase.

The elution profiles of the reaction mixture of daptomycin and activated dextran in a coupling pH range of 2–5 at 25 °C showed that the reaction mixtures contained at least two different molecular sizes. Fig. 4 was an example of elution profile of the reaction mixture at pH 2. The obvious shoulders of the peak implied that co-elution of macromolecules occurred. The elution volumes of 35 and 60 mL corresponded to about 40,000 and 1600 in molecular weights. The percent recovery of daptomycin and daptomycin conjugates using co-solvent mobile phase was

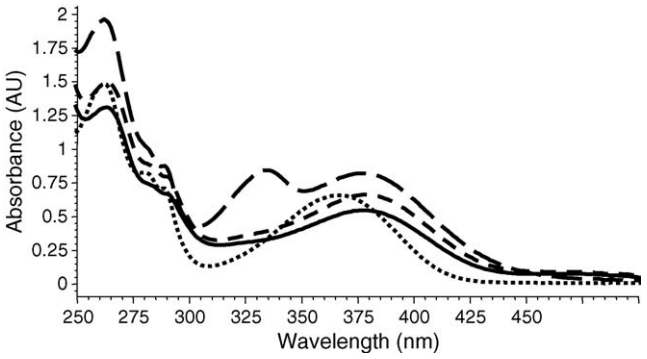

Fig. 10. UV spectra of daptomycin (···), fractions with elution volumes of 24 mL (—), 36 mL (- - -), and 62 mL (– –) in 10% acetonitrile in water after 0.5 mL of 0.015 M daptomycin and activated dextran coupling at reaction pH 2, 25 °C was applied on Sephadex G-100 column using 10% acetonitrile in water as a mobile phase. Fractions with elution volumes of 36 and 62 mL were diluted with 10% acetonitrile (dilution factor = 2).

96.9–99.6% versus 84% without non-aqueous solvent. Thus, adsorption of daptomycin on the column was minimized by using a co-solvent.

3.5. Spectral characteristics of fractions

UV and fluorescence properties of fractions from coupling pH 2–5 were investigated. The UV absorbance at 377 nm suggested that daptomycin was present in every fraction which had elution volume higher than 20 mL (Fig. 10). The UV absorbance at 377 nm corresponded to a bathochromic shift of the kynurenine absorption maximum. Characteristics of the UV spectra of small molecular weight fractions showed a bathochormic shift of the kynurenine absorption maxima and also possessed absorption maxima at about 330 nm.

Fluorescence properties of each fraction were studied using excitation and emission maxima of kynurenine; i.e. 365 and 465 nm, respectively. Kynurenine fluorescence enhancement (by 1.5–2.4-fold) was observed in fractions containing high molecular weight conjugates (Table 3). However, fluorescence intensity of kynurenine low molecular weight fractions was one-half of that of daptomycin at the same concentration.

Concentration of daptomycin present in each fraction was determined from the UV absorbance at 282 nm. The concentration of unconjugated daptomycin present in high molecular weight fractions was also estimated by HPLC analysis to be less than 10%. Fractions obtained at each reaction pH that possessed the same spectral properties were pooled together and lyophilized for further studies. No changes in UV and fluorescence characteristics of the reconstituted lyophilized conjugates were observed after the lyophilization process.

3.6. Characterization of daptomycin-activated dextran conjugates

The coupling reaction was hypothesized to be similar to the reaction between daptomycin and glyceraldehyde in which unprotonated primary amine of kynurenine reacted with aldehyde and formed various products including imines, anilide derivatives, and other unidentified compounds (Muangsiri et al., 2005).

Table 3
UV and fluorescence properties of daptomycin, two products from the reaction of daptomycin with glyceraldehyde (imine product and anilide product), and two molecular weight fractions from the reaction of daptomycin and activated dextran 40 (the high molecular weight fractions, and the low molecular weight fractions)

Compound	UV absorption maximum of kynurenine (nm)	Relative fluorescence intensity of kunurenine[a]
Daptomycin	365	1.00
Imine product (product A)	375	1.74
High molecular weight fractions, pH 2	377	2.34–1.87
High molecular weight fractions, pH 3	377	2.22–1.88
High molecular weight fractions, pH 5	377	1.87–1.72
Anilide product (product B)	330	0.570
low molecular weight fractions, pH 2	330	0.450
low molecular weight fractions, pH 3	330	0.650–0.510
low molecular weight fractions, pH 5	330	0.380

[a] Relative fluorescence intensity of the compound to that of kynurenine in daptomycin at the same concentration determined from the UV absorption at 282 nm.

High molecular weight fractions possessed a UV bathochormic shift and fluorescence enhancement of kynurenine which were consistent with the spectral properties of the imine product from the reaction of daptomycin and glyceraldehyde (Table 3). Unconjugated daptomycin, anilide derivatives, and unidentified compounds were co-eluted in the low molecular weight fractions. The presence of anilide products in the low molecular weight fractions was supported by evidence including UV and fluorescence characteristics. A proposed reaction scheme of anilide formation is shown in Fig. 11. The formation of anilide product in the reaction between daptomycin and activated dextran was likely to be a result of intramolecular hydrogen bonding leading to the bond cleavage of the carbinolamine intermediate at the side chain sugar. This mechanism was demonstrated to be plausible in the reaction between daptomycin and glyceraldehyde in which hydroxyl group of carbinolamine intermediate was in a close proximity to form hydrogen bond with another hydroxyl group of glyceraldehyde. Thus, anilide product was present in the low molecular weight fractions but absent in the high molecular weight fractions.

3.7. Determination of drug loading

The amounts of daptomycin conjugated to one gram of macromolecule were estimated to be 164, 167, and 141 mg at reaction pH values of 2, 3, and 5, respectively. In other words, the conjugation efficiency was one molecule of daptomycin for approximately 13, 13, and 15 aldehyde groups of activated dextran at reaction pH values of 2, 3, and 5, respectively.

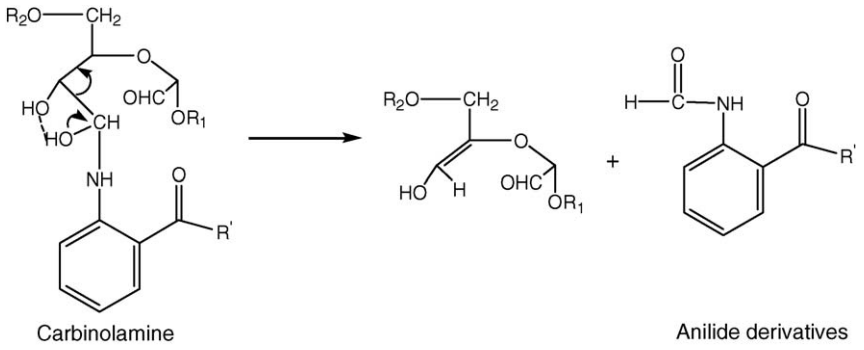

Fig. 11. Proposed reaction scheme of anilide derivative formation in the coupling reaction between kynurenine side chain of daptomycin (Ŕ) and activated dextran where R_1 and R_2 were glucose subunits of activated dextran. The anilide side chain formed from the kynurenine side chain of daptomycin.

3.8. In vitro drug release

The release of daptomycin from macromolecular conjugates prepared at pH 2 was investigated at 60 °C in pH 1, 4, and 7.4 buffer solutions (Table 2). The degradation of activated dextran at the experimental conditions was not observed using the current HPLC analysis. Concentration time profiles of free daptomycin showed degradation half-lives of 19, 26, and 26 h in buffer pH 1.0, 4.0, and 7.4, respectively. The release profiles of free daptomycin (coupling reaction at pH 2) showed the appearance and loss of free daptomycin in pH 1 and 4 release media (Fig. 12). The daptomycin release using pH 7.4 medium showed only loss of daptomycin. First-order plots of daptomycin degradation and release showed that the decrease in free daptomycin concentration in the release medium was due to daptomycin degradation; i.e. terminal slopes of the logarithmic transformed release profiles were 0.036 and 0.025 h^{-1} and the apparent rate constants of daptomycin loss were 0.036 and 0.026 h^{-1} at pH 1 and 4, respectively. Initial appearance rate for daptomycin was dependent on the release media pH. The initial rate was estimated to be 0.025 and 0.009 mM/h at pH 1 and 4, respectively.

The total percent daptomycin release was determined by comparing the area under the curve (AUC) daptomycin release profiles with the AUC of daptomycin loss when initial daptomycin concentration equaled to initial concentration of daptomycin conjugates. The equation was derived as followed:

$$\text{Total percent daptomycin release} = \frac{\text{AUC}_{0\to\infty} \times k \times V \times \text{MW} \times 100}{\text{wt}} \quad (2)$$

where $\text{AUC}_{0\to\infty}$ is area under the curve from time = 0 to infinity (Mh), k the observed degradation rate constant (h^{-1}), V volume of reaction solution (mL), MW the molecular weight of daptomycin, and wt is weight in mg of daptomycin.

At pH 1 (reaction #4, Table 2) and 4 (reaction #5, Table 2), the $\text{AUC}_{0\to\infty}$ values and observed daptomycin degradation rate constants were determined to be 0.0012 and 0.001 Mh and 0.036 and 0.026 h^{-1}, respectively. Therefore, percent of daptomycin released from the conjugates in pH 1 and 4 media was estimated to be 8.3 and 6.0%, respectively.

Daptomycin conjugates were expected to release free daptomycin over a period of time based on the reversible nature of imine product between daptomycin and glyceraldehyde reaction (Muangsiri et al., 2005). The lack of daptomycin release from daptomycin activated dextran conjugates was likely due to the presence of high concentrations of unreduced aldehyde, the presence of daptomycin products from other unidentified

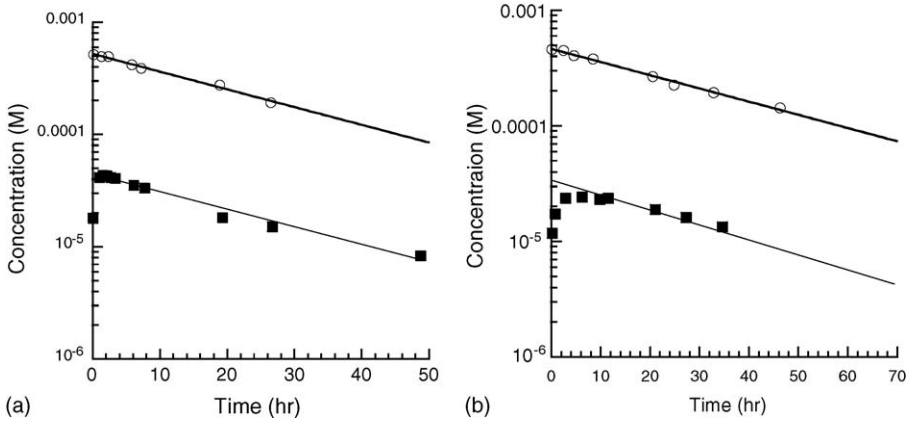

Fig. 12. Comparison of first-order plots of daptomycin (◯) degradation and daptomycin released from macromolecular conjugates (■) at 60 °C (a) in HCl/NaCl buffer pH 1 (μ = 0.154 M) (b) in acetate buffer pH 4 (μ = 0.154 M).

reaction pathways, or the further degradation of daptomycin conjugates by other pathways; for example, formation of hemiacetal or hemiketal from the reaction of aldehyde functional group with the hydroxyl side chain of serine (Lowry and Richardson, 1987; Chen et al., 2002).

3.9. Determination of fibrinogen–daptomycin conjugate binding by SPR

Volumes of 20 μL of daptomycin (200 nM), dextran 40 (200 nM), activated dextran 40 (200 nM), and macromolecular conjugates containing 855 nM of daptomycin were passed over the sensor chip surface in duplicate at a flow rate of 10 μL/min to determine the affinity for fibrinogen of each compound. Sensorgrams corrected for background are plotted in Fig. 13.

Dextran and activated dextran sensorgrams showed insignificant interactions with the human fibrinogen. However, free daptomycin and daptomycin conjugates sensorgrams showed significant interaction with human fibrinogen. In the free daptomycin sensorgrams, the signal increased from 0 to 30 RU within 10 s, reached a maximum response of about 40 RU then decreased to 10 RU after the introduction of the running buffer. The rapid decrease in signal in the dissociation phase indicated a high dissociation rate. Various models including one-to-one and parallel interaction models were used to fit the daptomycin sensorgrams (Karlsson and Faelt, 1997; Capila et al., 1999). The best fit was obtained with the parallel interaction model consistent with the trinodular structure of human fibrinogen containing two fragment D domains and one fragment E domain (Fig. 14a and Table 4). In the case of daptomycin human fibrinogen binding, the dissociation constants for daptomycin human fibrinogen binding were estimated to be 4.00×10^{-6} and 1.07×10^{-3} M using the parallel interaction model.

The sensorgrams of the daptomycin conjugates increased from 0 to 30 RU within 10 s of sample introduction. The signal reached a maximum of about 60 RU and then decreased during the dissociation phase. The dissociation kinetics were slower for the conjugates than observed with unconjugated daptomycin, which suggested that the conjugates adhered to human fibrinogen more tightly than daptomycin. The dissociation constants of the daptomycin conjugates were estimated by fitting the sensorgrams to various theoretical models including one-to-one, parallel interaction, and bivalent analyte models. The best fit was obtained with the bivalent analyte model which was consistent with the large molecular size of the conjugates and the presence of multiple potential ligands (daptomycin molecules) that may be able to bind to the binding sites of fibrinogen (Fig. 14b and Table 4).

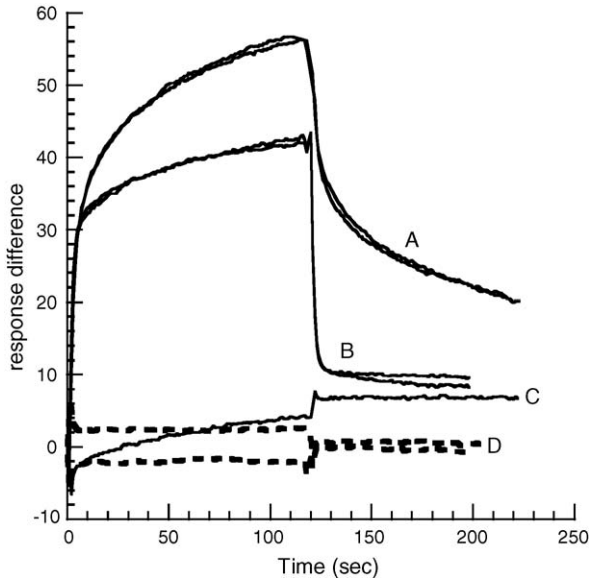

Fig. 13. Sensorgrams of macromolecular conjugates from conjugation pH 5 (A), 200 nM daptomycin (B), 200 nM activated dextran (C), and 200 nM dextran at the 20 μL injection volume, 10 μL/min flow rate on human albumin immobilized on the sensor chip CM5 using the BIAcore 3000.

Dissociation constants for daptomycin were somewhat lower (4.00×10^{-6} and 1.07×10^{-3} M) than that of the conjugates (1.68×10^{-4} M and 28.90 RU). Thus, binding affinity of daptomycin conjugates was greater than of unconjugated daptomycin.

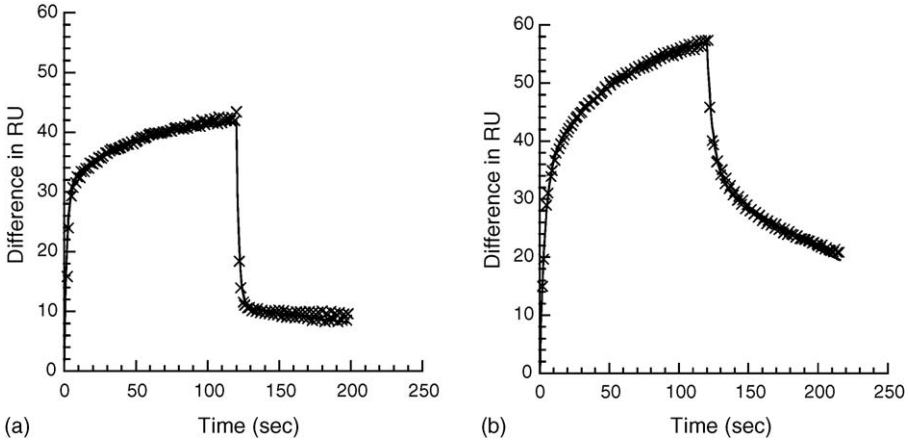

Fig. 14. Sensorgrams corresponding to (a) the interaction of 200 nM daptomycin with fibrinogen (×) using a flow rate of 10 μL/min fitted with the parallel interaction model (—) and (b) the interaction of 200 nM daptomycin conjugates with fibrinogen (×) using a flow rate of 10 μL/min fitted by the bivalent analyte model (—).

Table 4
Association and dissociation rate constants obtained by fitting sensorgrams of 200 nM daptomycin or daptomycin conjugates binding to fibrinogen to various models

Analyte	Model	k_{a1} ($s^{-1}M^{-1}$) (S.E.)	k_{d1} (s^{-1}) (S.E.)	k_{a2} ($s^{-1}M^{-1}$) (S.E.)	k_{d2} (s^{-1}) (S.E.)	χ^2
Daptomycin	One-to-one interaction model	1.68×10^3 (2.42×10^2)	1.94×10^{-2} (1.72×10^{-3})	–	–	7.28
	Parallel interaction model	8.96×10^2 (6.77×10^1)	5.21×10^{-1} (2.41×10^{-2})	4.89×10^2 (5.02×10^1)	3.59×10^{-3} (5.68×10^{-4})	0.47
Daptomycin conjugates	One-to-one interaction model	1.77×10^3 (4.65×10^1)	5.43×10^{-3} (1.64×10^{-4})	–	–	1.49
	Parallel interaction model	1.28×10^4 (8.56×10^1)	3.94×10^{-2} (1.64×10^{-4})	1.47×10^3 (5.88×10^1)	7.39×10^{-5} (1.32×10^{-4})	5.05
	Bivalent analyte model	1.27×10^3 (1.86×10^1)	2.13×10^{-1} (3.44×10^{-3})	1.09×10^{-4}[a] (2.59×10^{-6})	3.15×10^{-3} (4.37×10^{-5})	0.21

S.E., standard error.
[a] Unit: (response unit)$^{-1}$ s^{-1}.

4. Conclusion

In this study, a drug delivery system for daptomycin was made by forming macromolecular conjugates by reacting daptomycin and activated dextran. In a pH range of 2–5, the unprotonated primary amine of kynurenine ($pK_a = 0.8$) was likely to form an unstable imine bond with the aldehyde group of activated dextran and resulting in conjugate formation while the protonated form of ornithine primary amine ($pK_a = 10$) was likely inactive. The conjugates through the imine bond formation were expected to reversibly release daptomycin over a period of time.

Activation of dextran was achieved by periodate oxidation. The reaction went to the completion within 1 h at room temperature in the dark and was independent of dextran molecular weight. The extent of the oxidation reaction, number of aldehyde substitution on the activated dextran, could be controlled by manipulation of periodate concentration per glucose subunit present in the dextran. Every molecule of periodate was estimated to generate 1.65–1.72 aldehyde groups per glucose subunit.

Loss of daptomycin was increased from 10% (in the absence of activated dextran) to 90% in the presence of activated dextran. This suggested that daptomycin conjugates had been formed.

Separation of macromolecular conjugates was done by gel permeation chromatography using Sephadex G-100 as a stationary phase. 10% acetonitrile in water was used as a mobile phase to minimize non-specific adsorption of daptomycin on the stationary phase.

The elution profiles of the reaction mixture of daptomycin and activated dextran in a coupling pH range of 2–5 at 25 °C showed the presence of high molecular weight and low molecular weight compounds corresponding to about 40,000 and 1600 Da. High molecular weight fractions possessed UV and fluorescence characteristics similar to the spectral properties of the imine product from the reaction of daptomycin and glyceraldehyde. Spectral characteristics of low molecular weight fractions suggested the presence of anilide product.

Both daptomycin and daptomycin conjugates were shown to have affinity for human fibrinogen using SPR. Sensorgrams of daptomycin or daptomycin conjugates were best fit using a parallel interaction model or a bivalent analyte model, respectively. The parallel interaction model was consistent with the trinodular structure of fibrinogen resulting in the presence of two types of the binding sites available for daptomycin binding. The bivalent analyte model was consistent with the macromolecular structure of daptomycin conjugates whereby one molecule of conjugates could bind to more than one binding site of fibrinogen. Daptomycin conjugates appeared to possess relatively higher dissociation constants (1.68×10^{-4} M and 28.90 RU) than that of daptomycin (4.00×10^{-6} and 1.07×10^{-3} M).

The daptomycin conjugates regenerated daptomycin over a period of time in mildly acidic buffers (pH 1 and 4 at 60 °C). However, only about 9% of daptomycin released. It was speculated that the remaining excess aldehyde in daptomycin conjugates was responsible for the low release extent. Furthermore, daptomycin and activated dextran could form other products, which had not yet been identified, via other reaction pathways.

These products could be present in the fractions containing high molecular weight, imine product, and consequently the expected daptomycin release was over-estimated.

The objectives of this project were to synthesize and characterize daptomycin–dextran conjugates with respect to those biophysical properties (molecular size, release rate and fibrinogen binding) which were expected to enhance the pharmacokinetic properties of daptomycin. We were success in preparing conjugates with increased fibrinogen binding affinities and of appropriate size but the extent and rate of drug release was not adequate. Additional studies are underway to improve drug release and to evaluate other macromolecular carriers.

References

Akins, R.L., Rybak, M.J., 2001. Antimicrob. Agents Ch. 45, 454–459.

Alborn, W.E., Allen, N.E., Preston, D.A., 1991. Antimicrob. Agents Ch. 35, 2282–2287.

Battersby, J., Clark, R., Hancock, W., Puchulu-Campanella, E., Haggarty, N., Poll, D., Harding, D., 1996. J. Control. Release 42, 143.

Bergeron, M.G., 1986. Clin. Biochem. 19, 90.

Bingen, E., Doit, C., Lambert-Zechovsky, N., Tod, M., Petitjean, O., Bourgeois, F., Mariani-Kurkdjian, P., 1991. Eur. J. Clin. Microbiol. Infect. Dis. 10, 1062–1065.

Boaretti, M., Canepari, M., del Mar Lleo, M., Satta, G., 1993. Antimicrob. Agents Ch. 34, 1220–1226.

Capila, I., VanderNoot, V.A., Mealy, T.R., Seaton, B.A., Linhardt, R.J., 1999. FEBS Lett. 446, 327–330.

Chen, C.-W., Tsay, Y.-G., Wu, H.-L., Lee, C.-H., Chen, D.-S., Chen, P.-J., 2002. J. Biol. Chem. 277, 33058.

Debono, M., Abbott, B.J., Molloy, R.M., Fukuda, D.S., Hunt, A.H., Daupert, V.M., Counter, F.T., Ott, J.L., Carrell, C.B., et al., 1988. J. Antibiot. 41, 1093.

Domb, A.J., Linden, G., Polacheck, I., Benita, S., 1996. J. Polym. Sci. A Polym. Chem. 34, 1229–1236.

Domb, A.J., Benita, S., Polacheck, I., Linden, G., US6011008, 2000.

Dubrick, M.A., Wade, C.E., 1994. J. Trauma 36, 323–330.

Garrison, M.W., Vance-Bryan, K., Larson, T.A., Toscano, J.P., Rotschafer, J.C., 1990. Antimicrob. Agents Ch. 34, 1925.

Harada, M., Sakakibara, H., Yano, T., Suzuki, T., Okuno, S., 2000. J. Control. Release 69, 399–412.

Hemmelder, M.H., De Jong, P.E., De Zeeuw, D., 1998. J. Lab. Clin. Med. 132, 390.

Inman, E.L., Kirsch, L.E., European Patent Applied (Lilly, Eli, and Co., USA), EP, 1990, 14 pp.

Karlsson, R., Faelt, A., 1997. J. Immunol. Methods 200, 121–133.

Kim, D.S., Jung, Y.J., Kim, Y.M., 2001. Drug Dev. Ind. Pharm. 27, 97.

Kirsch, L.E., Molloy, R.M., Debono, M., Baker, P., Farid, K., 1989. Z. Pharm. Res. 6, 387.

Lamp, K.C., Rybak, M.J., Bailey, E.M., Kaatz, G.W., 1992. Antimicrob. Agents Ch. 36, 2709.

Lee, B.L., Sachdeva, M., Chambers, H.F., 1991. Antimicrob. Agents Ch. 35, 2505.

Logeart-Avramoglou, D., Jozefonvicz, J., 1999. J. Biomed. Mater. Res. (Appl. Biomater.) 48, 578–590.

Louie, A., Kaw, P., Liu, W., Jumbe, N., Miller, M.H., Drusano, G.L., 2001. Antimicrob. Agents Ch. 45, 845–851.

Lowry, T.H., Richardson, K.S., 1987. Mechanism and Theory in Organic Chemistry, 3rd ed.

Marchi, R., Mirshahi, S.S., Soria, C., Mirshahi, M., Zohar, M., Collet, J.P., de Bosch, N.B., Arocha-Pinango, C.L., Soria, J., 2000. Thromb. Res. 99, 187.

Michiels, M.J., Bergeron, M.G., 1996. Antimicrob. Agents Ch. 40, 203–211.

Mihara, K., Sawai, K., Takakura, Y., Hashida, M., 1994. Biol. Pharma. Bull. 17, 296–301.

Muangsiri, W., Kirsch, L.E., 2001. J. Pharm. Sci. 90, 1066.

Muangsiri, W., Kearney, W.R., Teesch, L.M., Kirsch, L.E., 2005. Int. J. Pharm. 289, 133.

Murray, B.E., 2000. New Eng. J. Med. 342, 710.

Nichifor, M., Coessens, V., Schacht, E.H., 1995. J. Bioactive Compatible Polym. 10, 199–222.

Retzinger, G.S., Deanglis, A.P. PCT Int. Appl. (University of Cincinnati, USA). WO, 1999, 62 pp.

Retzinger, G.S., DeAnglis, A.P., Patuto, S.J., 1998. Arterioscl. Throm. Vasc. 18, 1948.

Rybak, M.J., Bailey, E.M., Lamp, K.C., Kaatz, G.W., 1992. Antimicrob. Agents Ch. 36, 1109.

Rybak, M.J., Hershberger, E., Moldovan, R., Richard, G., 2000. Antimicrob. Agents Ch. 44, 1062–1066.

Sakamoto, N., Shioya, T., Serizawa, T., Akashi, M., 1999. Bioconj. Chem. 10, 538–543.

Snydman, D.R., Jacobus, N.V., McDermott, L.A., Lonks, J.R., Boyce, J.M., 2000. Antimicrob. Agents Ch. 44, 3447–3450.

Tally, F.P., DeBruin, M.F., 2000. J. Antimicrob. Chemo. 46, 523–526.

Vance-Bryan, K., Larson, T.A., Rotschafer, J.C., Toscano, J.P., 1992. Antimicrob. Agents Ch. 36, 2334–2337.

Wilson, W.R., Karchmer, A.W., Dajani, A.S., Taubert, K.A., Bayer, A., Kaye, D., Bisno, A.L., Ferrieri, P., Shulman, S.T., Durack, D.T., 1995. JAMA 274, 1706.

Woodworth, J.R., Nyhart Jr., E.H., Brier, G.L., Wolny, J.D., Black, H.R., 1992. Antimicrob. Agents Ch. 36, 318–325.

Yura, H., Yoshimura, N., Hamashima, T., Akamatsu, K., Nishikawa, M., Takakura, Y., Hashida, M., 1999. J. Control. Release 57, 87.

Zhao, H.H.N.D., 1991. Pharm. Res. 8, 400.

Zhao, Q., Tolmachev, V., Carlsson, J., Lundqvist, H., Sundin, J., Janson, J.C., Sundin, A., 1999. Bioconj. Chem. 10, 938.